

Kinetics and Mechanism of the Peroxidase-Catalyzed Iodination of Tyrosine[†]

Weimei Sun and H. Brian Dunford*

Department of Chemistry, University of Alberta, Edmonton, Alberta, Canada T6G 2G2

Received September 3, 1992; Revised Manuscript Received December 2, 1992

ABSTRACT: The kinetics of iodination of tyrosine by hydrogen peroxide and iodide, catalyzed by both horseradish peroxidase (HRP) and lactoperoxidase (LPO), were studied. The initial rates of formation of both molecular I_2 and moniodotyrosine (MIT) were measured with stopped flow techniques. The following reactions occur in both systems. Enzymatic: $Fe^{III} + H_2O_2 \rightarrow Fe^V=O + H_2O$; $Fe^V=O + I^- \rightarrow Fe^{III}-O-I^-$; $Fe^{III}-O-I^- + H^+ \rightarrow Fe^{III} + HOI$; $Fe^{III}-O-I^- + I^- + H^+ \rightarrow Fe^{III} + I_2 + HO^-$. Iodine equilibria: $I_2 + I^- \rightleftharpoons I_3^-$; $I_2 + H_2O \rightleftharpoons HOI + I^- + H^+$. Nonenzymatic iodination, one or both of the following: $Tyr + HOI \rightarrow MIT + H_2O$; $Tyr + I_2 \rightarrow MIT + I^- + H^+$, where Fe^{III} is native peroxidase, $Fe^V=O$ is compound I and Tyr is tyrosine. The big difference in the two systems is that the following reaction also occurs with LPO: $Fe^{III}-O-I^- + Tyr \rightarrow MIT + Fe^{III} + HO^-$, which is the dominant mechanism of iodination for the mammalian enzyme. The overall rate of formation of MIT is about 10 times faster for LPO compared to HRP under comparable conditions. A small decrease in rate occurs when D-tyrosine is substituted for L-tyrosine in the LPO reaction. Thus LPO has a tyrosine binding site near the heme. A kinetically controlled maximum is observed in I_3^- concentration. Once equilibrium is established, I_2 is the dominant form of inorganic iodine in solution. However, hypiodous acid may be the inorganic iodination reagent.

Because of the physiological significance of tyrosine iodination, several studies have been devoted to the peroxidase catalysis of this reaction. There are conflicting reports in the literature with respect to the iodination mechanism. The main conflict centers upon the identity of the iodinating species. Although it was suggested that I_2 is an obligatory intermediate (Thomas & Hager, 1969), there is evidence indicating that I_2 is not the active iodinating agent in thyroid peroxidase-catalyzed iodination (Taurog, 1970). Other experimental results support the conclusion that iodination does not occur by way of free I_2 , but rather via an iodinating species associated with the enzyme (Bayse & Morrison, 1971; Pommier et al., 1973; Davidson et al., 1978). It has been suggested that the iodinating species is enzyme-activated hypiodous acid, HOI, on the basis of a kinetic analysis of tyrosine iodination catalyzed by HRP¹ at low pH (Dunford & Ralston, 1983). Magnusson et al. (1984a) claimed that free HOI is the active iodinating species in the LPO iodination system. A proposal has been made that both I_2 and HOI may play roles as iodinating agents (Huwiler et al., 1985). The effect of iodide on the interconversion of oxidized enzyme species has been studied for lactoperoxidase and thyroid peroxidase (Kohler et al., 1988). Huber et al. (1989) concluded that a highly reactive iodinating intermediate is produced on lactoperoxidase, which diffuses from the enzyme before reacting.

The experiments described here were designed to study further the possible iodinating species in mixtures of hydrogen peroxide, iodide, and tyrosine catalyzed by two different enzymes: the plant enzyme horseradish peroxidase (HRP; donor, H_2O_2 oxidoreductase, EC 1.11.1.7) and the mammalian enzyme lactoperoxidase (LPO; donor, H_2O_2 oxidoreductase, EC 1.11.1.7). The initial rates of formation of I_2 and MIT

were measured at 460 nm [ϵ_{I_2} 7.46×10^2 M⁻¹ cm⁻¹ (Awtrey & Connick, 1951)] and at 290 nm [ϵ_{MIT} 2.30×10^3 M⁻¹ cm⁻¹ (Figure 1)], using the stopped-flow technique. Initial rates of I_2 formation were compared in the presence of tyrosine and in blank experiments without tyrosine present. It is shown that different mechanisms are required in order to describe the two different enzyme-catalyzed iodination reactions.

In the peroxidase-catalyzed iodination of tyrosine, the first step is the reaction of the native enzyme with H_2O_2 to form compound I, which contains two more oxidizing equivalents than the native enzyme. This compound is able to oxidize an electron donor in a one-electron or two-electron transfer reaction. It has been shown that the oxidation of iodide by enzyme compound I is a two-electron transfer process. Iodide is oxidized to an oxidation state of +1 and compound I is reduced directly to the native enzyme (Roman & Dunford, 1972). The direct oxidation of tyrosine is a one-electron transfer process in which compound I is reduced to compound II and a tyrosyl radical is generated (Ralston & Dunford, 1978). The oxidations of both iodide and tyrosine by HRP-I are strongly pH dependent. The HRP-I reaction with iodide is much faster in the pH 3–4 region than at alkaline pH (Roman & Dunford, 1972), whereas the reaction of HRP-I with tyrosine reaches a maximum at pH 9.6 (Ralston & Dunford, 1978). In order to minimize the direct oxidation of tyrosine and maximize the oxidation of iodide, we used a pH of 3.60 for the HRP system. For LPO, we used the same pH for optimal rate of iodination observed by Morrison and Bayse (1970): pH 5.0.

MATERIALS AND METHODS

Materials. Horseradish peroxidase was purchased as an ammonium sulfate suspension from Boehringer-Mannheim. After dialysis against deionized water from the Milli-Q system, a purity number of 3.25–3.40 was determined from the ratio of absorbances at 403 and 280 nm. The concentration of the enzyme solution was measured spectrophotometrically at 403 nm, where the molar absorptivity is 1.02×10^5 M⁻¹ cm⁻¹ (Ohlsson & Paul, 1976). Lactoperoxidase with a purity

[†] This work was supported in part by grants from the Natural Science and Engineering Research Council of Canada.

* Correspondence should be addressed to this author.

¹ Abbreviations: HRP, horseradish peroxidase; HRP-I, horseradish peroxidase compound I; HRP-II, horseradish peroxidase compound II; HRP-O-I⁻, horseradish peroxidase bound hypiodite; LPO, lactoperoxidase; LPO-I, lactoperoxidase compound I; LPO-O-I⁻, lactoperoxidase bound hypiodite; MIT, moniodotyrosine; DIT, diiodotyrosine.

number (A_{412}/A_{280}) of 0.85 was purchased from Sigma as a purified, lyophilized powder. Its concentration was determined using a molar absorptivity of $1.12 \times 10^5 \text{ M}^{-1} \text{ cm}^{-1}$ at 412 nm (Paul & Ohlsson, 1985).

The concentration of hydrogen peroxide, obtained from BDH Chemicals, was determined after appropriate dilution using the horseradish peroxidase assay (Cotton & Dunford, 1973). L- and D-tyrosine, MIT, and DIT were purchased from Sigma. Stock solutions of tyrosine, MIT, and DIT ($\sim 2.8 \text{ mM}$) were prepared by dissolution in appropriate volumes of 0.1 M KOH and then neutralizing the solutions by adding the same volumes of 0.1 M HNO_3 . Reagent grade potassium iodide was purchased from Shawinigan Chemicals. All the chemicals were used without further purification. Solution concentrations were determined by weight and fresh stock solutions were prepared just before use.

Chemicals for the phosphate and citrate buffers were reagent grade and used without further purification. The ionic strength of the buffers were 0.01 M . Analytical reagent K_2SO_4 , obtained from AnalaR, was used to keep the total ionic strength of reaction mixtures at 0.11 M .

All solutions were prepared using deionized water obtained from the Milli-Q system (Millipore).

Methods. Optical absorption measurements on a conventional time scale ($>1 \text{ s}$) were made on a Cary 219 spectrophotometer. Stopped-flow and rapid scan experiments were performed on a Photol (formerly Union Giken) model RA-601 rapid reaction analyzer. O_2 production was determined with a Yellow Spring Instruments model 53 oxygen monitor.

A pH-jump method was used for all stopped-flow experiments because the native HRP and LPO are not stable at low pH; we illustrate for measurement of rate constants involving HRP-I. One cuvette contained stable HRP-I (1:1 ratio of H_2O_2 and HRP) in phosphate buffer of ionic strength 0.01 M , pH 6.17 (total ionic strength 0.11 M); the other cuvette contained iodide (and tyrosine except for blank experiments) in citrate buffer, pH 3.23; ionic strength 0.11 M . After the two solutions were mixed, the final pH was 3.60. A Fisher Accumet model 420 digital pH meter was used for pH measurements.

The absorbance scale of the single-beam Photol rapid reaction analyzer was calibrated using the stopped-flow mode at 353 nm . Different concentrations of I_3^- solutions were made by dissolving a small amount of crystalline I_2 with a relatively large amount of KI in pH 3.60 citrate buffer. The absolute absorbances, A , of these solutions were measured on a Cary 219 spectrophotometer at 353 nm . On the Photol instrument, pH 3.60 citrate buffer was used as a reference to adjust the baseline to a certain absorbance, A_b , and the relative absorbances, A_r , of the above I_3^- solutions were measured. Therefore ΔA , which is equal to $A_r - A_b$, could be obtained. A calibration curve was made by plotting ΔA against the absolute absorbance A for different concentrations of I_3^- . All experiments were performed at $25.0 \pm 0.1^\circ \text{C}$.

RESULTS

Spectra of L-Tyrosine, MIT, and DIT. Figure 1 shows the optical spectra of L-tyrosine, MIT, and DIT at pH 3.60. An isosbestic point of MIT and DIT occurs at 292 nm . The biggest absorbance difference between MIT and tyrosine occurs at 290 nm where a molar absorptivity value of $2.30 \times 10^3 \text{ M}^{-1} \text{ cm}^{-1}$ was obtained for MIT, while tyrosine shows almost no absorbance at this wavelength. Similar spectra were obtained at pH 4.97.

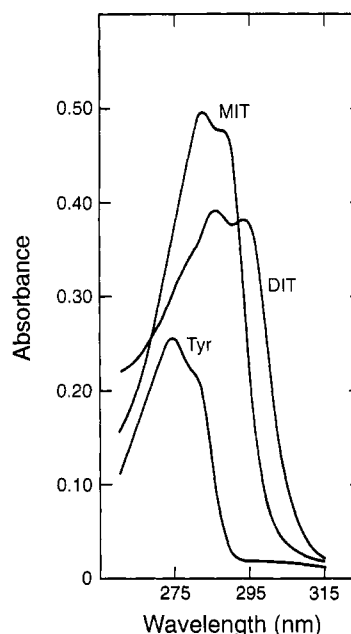


FIGURE 1: Optical spectra of 0.20 mM L-tyrosine, 0.20 mM moniodotyrosine, and 0.20 mM diiodotyrosine in citrate buffer of ionic strength 0.11 M , pH 3.60, at 25°C .

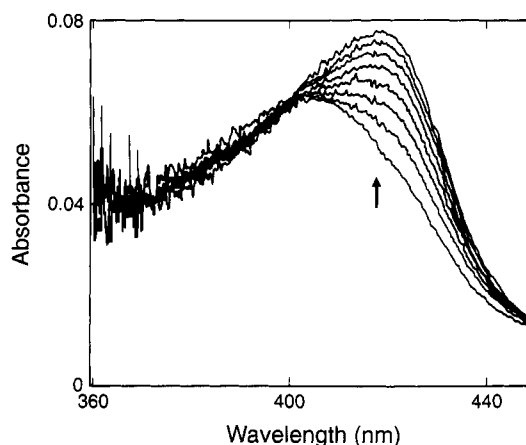


FIGURE 2: Rapid scan spectra over 8.3 s for the reaction of $1.14 \mu\text{M}$ HRP-I with $16.7 \mu\text{M}$ L-tyrosine at pH 3.60. One cuvette contained HRP-I in phosphate buffer, pH 6.17, total ionic strength 0.11 M ; the other contained L-tyrosine in citrate buffer, pH 3.23, ionic strength 0.11 M . The final pH was 3.60. The partial conversion of HRP-I to HRP-II is shown clearly. The arrow indicates the direction of absorbance change with increasing time.

HRP Results

Rate of Conversion of HRP-I to HRP in the Presence of Iodide and/or Tyrosine. Figure 2 shows the rapid scan spectra for the reaction of HRP-I with tyrosine at pH 3.60. The partial conversion of HRP-I to HRP-II is observed, i.e., the start of a one-electron reduction of HRP-I.

In marked contrast, Figure 3 shows the rapid scan spectra during the conversion of HRP-I in the presence of both KI and tyrosine at pH 3.60. These spectra are very similar to those obtained when tyrosine is absent. Over a period of 80 ms , HRP-I is going directly to native HRP, i.e., only iodide is reacting with HRP-I, and the iodide is converted to a +1 oxidation state.

Rate constants of the reaction of HRP-I with iodide were measured at 403 nm without and with tyrosine present at pH 3.60 as a function of iodide concentration. Linear plots of the pseudo-first-order rate constants were obtained, and from the slopes the second-order rate constants for the reaction of HRP-I

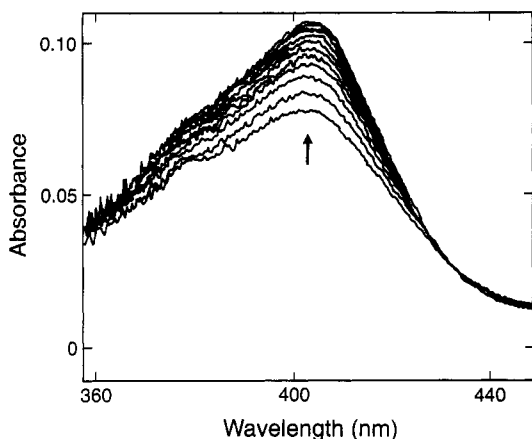
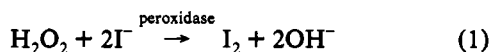


FIGURE 3: Rapid scan spectra over 80 ms during the direct conversion of 1.14 μM HRP-I to native HRP in the presence of both 17.2 μM KI and 17.2 μM L-tyrosine at pH 3.60. Other experimental conditions are as given in the legend to Figure 2. The results indicate that the only reaction is the two-electron transfer from iodide to HRP-I.

with iodide could be obtained. The results are $(1.8 \pm 0.2) \times 10^6 \text{ M}^{-1} \text{ s}^{-1}$ without tyrosine present and $(1.9 \pm 0.2) \times 10^6 \text{ M}^{-1} \text{ s}^{-1}$ with tyrosine present, which are identical within experimental error. Hence, it was confirmed that tyrosine does not affect the reaction of HRP-I with iodide at pH 3.60.

Steady-State Experiments. (1) *The Time Dependences of I_3^- , I_2 , and I^- Concentrations in the Iodination Reaction from the Stopped-Flow Experiments.* Iodide has no absorption in the region 265–500 nm. Tyrosine has its maximum absorbance at 274 nm (Figure 1). Triiodide ion has absorbance maxima at 353, 287.5, and 460 nm [$\epsilon_{353} = 2.64 \times 10^4 \text{ M}^{-1} \text{ cm}^{-1}$, $\epsilon_{287.5} = 4.00 \times 10^4 \text{ M}^{-1} \text{ cm}^{-1}$, and $\epsilon_{460} = 9.75 \times 10^2 \text{ M}^{-1} \text{ cm}^{-1}$ (Awtrey & Connick, 1951)]. Iodine has its maximum absorbance at 460 nm [$\epsilon_{460} = 7.46 \times 10^2 \text{ M}^{-1} \text{ cm}^{-1}$ (Awtrey & Connick, 1951)]. The biggest absorbance difference between MIT and tyrosine is at 290 nm where $\epsilon_{\text{MIT}} = 2.30 \times 10^3 \text{ M}^{-1} \text{ cm}^{-1}$, while tyrosine does not have any absorption at this wavelength, as shown in Figure 1. Figure 4 shows stopped flow traces at 353 (a), 460 (b), and 290 nm (c) obtained from the reaction mixture containing 1.14 μM HRP, 1.02 mM H_2O_2 , 324 μM KI, and 324 μM tyrosine in pH 3.60 citrate buffer with ionic strength of 0.11 M. Hence, curve a is the time course for I_3^- at its maximum absorbance of 353 nm. By using the calibration curve which was obtained for the Photol instrument, the relative absorbances obtained from curve a could be converted to I_3^- concentrations. The results shown in Figure 5a indicate that a kinetically controlled maximum occurs in I_3^- concentration. The fast enzymatic oxidation of I^- to HOI is followed by reaction of HOI with I^- to generate I_2 ; the overall process is shown in eq 1. The I_2 in turn reacts with excess I^- to form I_3^- (eq 2).



It follows that

$$K_2 = \frac{[\text{I}_3^-]}{[\text{I}_2][\text{I}^-]} = \frac{k_1}{k_2} = 729 \text{ M}^{-1} \quad (3)$$

$$[\text{I}^-]_{\text{total}} = [\text{I}^-] + 2[\text{I}_2] + 3[\text{I}_3^-] \quad (4)$$

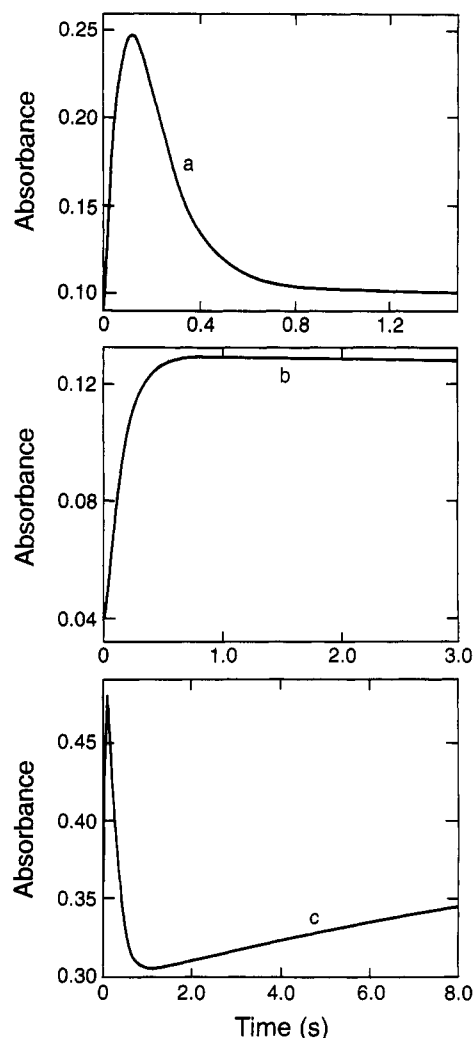


FIGURE 4: Formation and disappearance of I_3^- and I_2 and formation of MIT during the HRP-catalyzed iodination of tyrosine: (a) I_3^- measured at 353 nm; (b) I_2 measured at 460 nm, and (c) MIT measured at 290 nm. Initial concentrations are $[\text{KI}] = [\text{tyrosine}]$, 324 μM ; $[\text{H}_2\text{O}_2]$, 1.02 mM; $[\text{HRP}]$, 1.14 μM . One cuvette contained H_2O_2 and L-tyrosine in citrate buffer, pH 3.50, ionic strength 0.11 M; the other contained KI and HRP in K_2SO_4 solution of ionic strength 0.11 M. The final pH was 3.50.

The thermodynamics of the formation of I_3^- have been extensively studied; reported values of K_2 are 768 M^{-1} (Davies & Gwynne, 1952), 721 M^{-1} (Ramette & Sandford, 1965), 698 M^{-1} (Palmer et al., 1984), and 746 M^{-1} (Wren et al., 1986), within the experimental error in eq 3. Using the measured I_3^- concentrations and combining the equilibrium constant of eq 3 with the mass conservation in eq 4, the corresponding I^- and I_2 concentrations at different times were calculated. The results shown in Figure 5b clearly show that, once equilibrium is established, molecular I_2 is the dominant form of inorganic iodide in the solution. Therefore, in curve b of Figure 4, the absorbance at 460 nm at times less than 400 ms is attributable to a mixture of I_2 and I_3^- . In order to determine an accurate initial rate of I_2 formation, the tangent from the starting point of curve b was taken because at that point only I_2 has been formed without any interference of I_3^- (Figure 4). At times longer than 1.0 s, it was observed that the absorbance at 460 nm decreases, which indicated that I_2 is being consumed. The time course of 290 nm in curve c of Figure 4 shows that the absorbance increases after 1.0 s, which is caused by MIT formation without any interference from I_3^- . By using the tangent from the starting point of this increase in absorbance in curve c, the initial rate of MIT formation

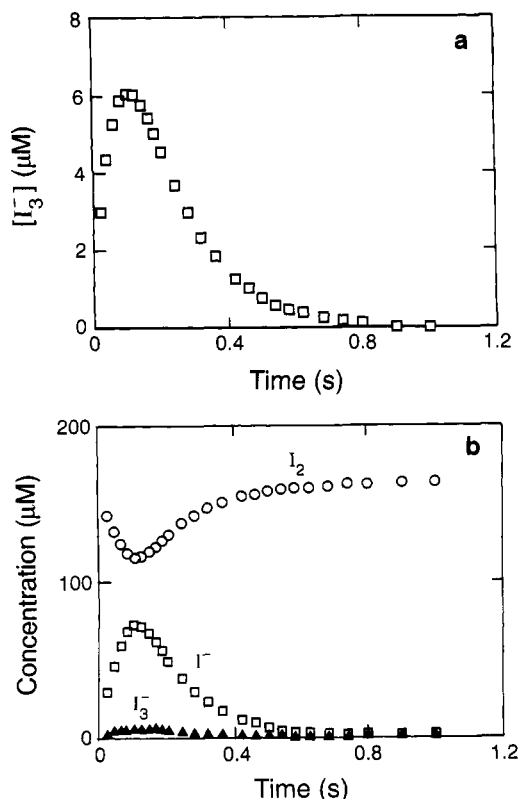


FIGURE 5: (a) I_3^- concentration over a period of 1.2 s in the reaction mixture of 1.14 μM HRP, 1.02 mM H_2O_2 , 324 μM KI, and 324 μM tyrosine at pH 3.60. (b) Comparison of time dependences of the concentrations of I_3^- , I^- , and I_2 . Conditions are as in panel a.

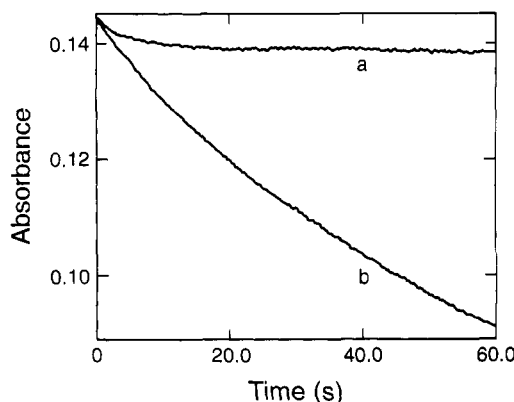


FIGURE 6: Disappearance of I_2 monitored over 60 s at 460 nm in a reaction mixture of HRP, H_2O_2 , and KI in the absence (curve a) and presence (curve b) of tyrosine at pH 3.60 (as shown in Figure 6). Curve a shows a small decrease of I_2 in the absence of tyrosine caused by the pseudocatalytic reaction of HRP (see later). Curve b shows the much larger decrease in I_2 in the presence of tyrosine.

could be obtained accurately. Overall, from the results of Figures 4 and 5b, we conclude that the iodination reaction coincides with depletion of the I_2 concentration.

Stopped-flow experiments were used to monitor the disappearance of I_2 at 460 nm. Results over a 60 s span are shown in the absence (curve a) and presence (curve b) of tyrosine at pH 3.60 (as shown in Figure 6). Curve a shows a small decrease of I_2 in the absence of tyrosine caused by the pseudocatalytic reaction of HRP (see later). Curve b shows the much larger decrease in I_2 in the presence of tyrosine.

(2) O_2 Production from Degradation of H_2O_2 . Several investigators have reported that the so-called pseudocatalytic degradation of H_2O_2 was detected in the lactoperoxidase iodination system (Magnusson & Taurog, 1983; Magnusson et al., 1984b; Huwiler & Kohler, 1984; Huwiler et al., 1985).

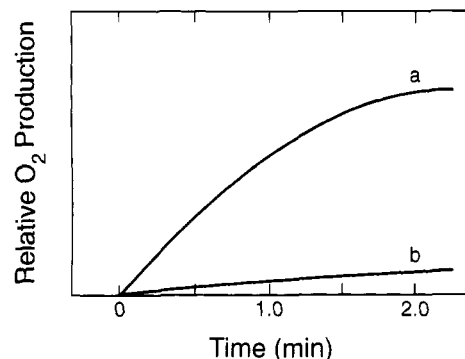


FIGURE 7: Relative O_2 production in a reaction mixture of 324 μM KI, 2.03 mM H_2O_2 , and 2.27 μM HRP, curve a, and same reaction mixture with 324 μM tyrosine added, curve b. Citrate buffer pH 3.60.

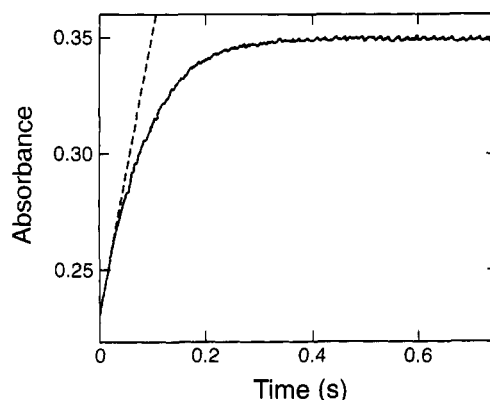
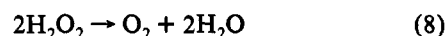
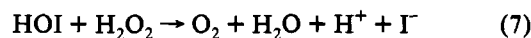
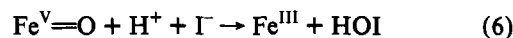
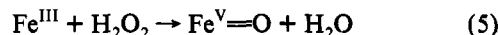


FIGURE 8: Formation of I_2 monitored at 460 nm in a reaction mixture of 324 μM KI, 324 μM tyrosine, 1.02 mM H_2O_2 , and 1.14 μM HRP at pH 3.60. The initial rate was determined from the tangent to the curve.

The experiments described here were designed to study this phenomenon in the HRP iodination system. Under steady-state conditions with KI, H_2O_2 , and HRP present, curve a of Figure 7 shows that a large amount of O_2 was produced. In contrast, when tyrosine was present, the catalytic-like reaction was markedly inhibited, as shown in curve b. This indicated that H_2O_2 was utilized primarily for iodination in the presence of tyrosine, even though the degradation of excess H_2O_2 by hypiodous acid, HOI, was still competing with the tyrosine iodination. The pseudocatalytic reaction can be explained as follows:

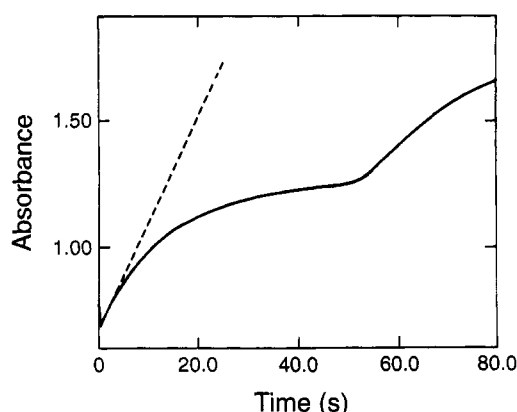


where Fe^{III} represents native HRP and $Fe^V=O$ HRP-I.

(3) Effect of I^- Concentration on the Initial Rates of Formation of I_2 and MIT. The steady-state conditions were changed by increasing the iodide concentration and hence the $[I^-]/[Tyr]$ ratio. All experiments were carried out by keeping the concentrations of tyrosine, H_2O_2 , and HRP constant. The $[I^-]/[Tyr]$ ratio was varied over the range 1:1 to 6:1. Figure 8 shows a representative time course at 460 nm for 750 ms and the initial rate of I_2 formation for an $[I^-]/[Tyr]$ ratio of 1:1. Data for all $[I^-]/[Tyr]$ ratios are collected in Table I.

Table I: Dependence of the Initial Rates of I_2 and MIT Formation on I^- Concentrations for HRP and LPO Iodination Systems^a

$[I^-]$ (mM)	I ₂ formation rate (M s ⁻¹)		MIT formation rate (M s ⁻¹)	
	HRP (× 10 ³)	LPO (× 10 ³)	HRP (× 10 ⁵)	LPO (× 10 ⁴)
0.324	0.62	2.20	0.44	0.37
0.648	1.23	2.16	0.89	1.04
0.972	1.61	2.25	1.42	2.15
1.13				2.88
1.30	1.94	2.21	2.32	3.66
1.46				5.40
1.62	2.24	2.16	3.05	5.98
1.78		2.10		4.99
1.94	2.47	2.09	4.19	

^a [HRP] or [LPO], 1.14 μM; [H₂O₂], 1.02 mM; [Tyr], 324 μM.FIGURE 9: Formation of MIT (and subsequent reaction) monitored over 80 s at 290 nm in a reaction mixture of 1.14 μM HRP, 1.02 mM H₂O₂, 324 μM tyrosine, and 1.29 mM KI (i.e., a $[KI]/[Tyr]$ ratio of 4.0) at pH 3.50. The initial rate was determined from the tangent to the first phase.

For the same experimental conditions, the time courses at 290 nm were measured. As the ratio of the $[I^-]/[Tyr]$ increased from 1:1 to 4:1, the absorbance trace at 290 nm over 80 s was observed to change from a monophasic to a biphasic curve. Figure 9 shows the curve for the $[I^-]/[Tyr]$ ratio of 4:1 in the HRP system. The initial rate of MIT formation was obtained by constructing the tangent from the starting point of the first phase as shown. The second phase might be due to the mixture of the second product DIT and I_3^- . The initial rates of MIT formation were determined as the $[I^-]/[Tyr]$ ratio increased. Data are shown in Table I.

(4) *The Effect of Tyrosine on I_2 Formation.* Experiments were performed to investigate I_2 formation in the presence and absence of tyrosine. The initial rates of I_2 formation are collected in Table II. The rates of I_2 formation are almost the same with and without tyrosine present.

LPO Results

Steady-state Experiments. (1) *Effect of I^- Concentration on the Initial Rates of Formation of I_2 and MIT.* The same steady-state conditions were used as for the HRP iodination system except that the pH was 4.97. The results are displayed in Figure 10. Absorbance at 353 nm reflects the concentration of I_3^- . The 290-nm results show interference from I_3^- absorbance if I_3^- is present; in its absence, they are an accurate measure of MIT concentration. There is an initial burst in I_3^- formation followed by its rapid disappearance as the equilibrium in eq 2 is established. For a 4.5:1 ratio of $[KI]/[Tyr]$ or lower, the absorbance of I_3^- falls effectively to zero and remains there, whereas MIT formation is occurring. This

Table II: Effect of Tyrosine on the Initial Rate of I_2 Formation for HRP and LPO Systems^a

$[I^-]$ (mM)	I ₂ formation rate (× 10 ³ M s ⁻¹)			
	HRP		LPO	
	with Tyr present	without Tyr present	with Tyr present	without Tyr present
0.324	0.62	0.72	2.20	10.3
0.648	1.23	1.33	2.16	9.69
0.972	1.61	1.60	2.25	10.2
1.30	1.94	1.78	2.21	9.57
1.62	2.24	2.04	2.16	9.76
1.78		2.26	2.10	9.24
1.94	2.47	2.44	2.09	8.92

^a Concentrations as in Table I.

shows clearly that I_3^- is not the iodinating species. For higher ratios of $[KI]/[Tyr]$, the results in Figure 10 show some reformation of I_3^- in later stages of the reaction. There is a lag phase in I_3^- reformation which is made shorter by higher ratios of $[KI]/[Tyr]$. During the lag phase, initial rates of MIT formation can be measured without interference from I_3^- absorbance. Hence, it is ensured that the measurement of the initial rate of MIT formation at 290 nm was accurate, i.e., without any interference of the I_3^- in the limited range of I^- concentration used in this study. We did not attempt to measure rates for $[KI]/[Tyr]$ greater than 5.5:1, where the re-formation of I_3^- could not be distinguished from MIT formation. As is explained below, the initial rates of MIT formation are a true measure of the LPO-catalyzed reaction and the re-formation of I_3^- in the later stages is indicative of nonenzymatic iodination which occurs when all H₂O₂ is consumed.

The same method used to determine the initial rate of I_2 formation for HRP was applied for LPO as well. The initial rates of I_2 formation were determined as the $[I^-]/[Tyr]$ increased from 1:1 to 6:1. Data are collected in Table I. Comparison plots of the rates of I_2 formation versus the $[I^-]/[Tyr]$ ratio for the two systems are displayed in Figure 11a. Under the same experimental conditions, the time courses at 290 nm were measured. The initial rates of MIT formation were determined as the $[I^-]/[Tyr]$ ratio increased by the same method used for HRP. These data are also shown in Table I. The overall rate of formation of MIT is about 10 times faster for LPO compared to HRP under comparable conditions. Comparison plots of the rates of MIT formation versus the $[I^-]/[Tyr]$ ratio for the two systems are shown in Figure 11b. Inhibition of MIT formation was observed in the LPO system as the $[I^-]/[Tyr]$ ratio increased to 5.5:1.

(2) *The Effect of Tyrosine on I_2 Formation.* Experiments in the presence and absence of tyrosine were also carried out for LPO. The initial rates of I_2 formation were measured as the $[I^-]$ changed from 324 μM to 1.94 mM. Data are collected in Table II. The rates of I_2 formation are about 5 times faster without tyrosine present for LPO than when tyrosine was present. Thus when LPO is used, tyrosine is an effective competitor for the I_2 precursor. The HRP results, where the presence or absence of tyrosine had little or no effect on I_2 formation, are in sharp contrast.

(3) *Iodination of D-Tyrosine.* Measurements have been made under the same experimental conditions using D-tyrosine instead of L-tyrosine in the LPO-catalyzed reaction. The results are shown in Table III. It was observed that D-tyrosine is less reactive in MIT formation; this leads to more I_2 formation.

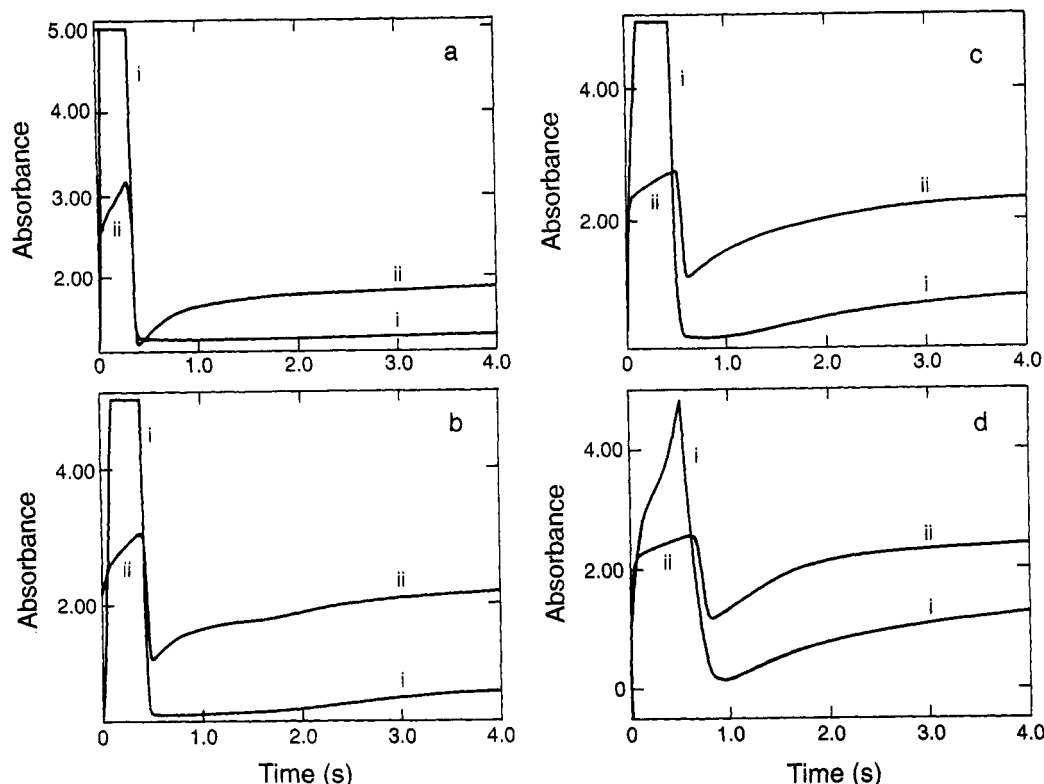


FIGURE 10: Absorbances at 353 and 290 nm for the LPO-catalyzed iodination of tyrosine. The measurements at 353 nm (i) are proportional to the concentration of I_3^- . Measurements at 290 nm (ii) reflect the concentration of MIT but are interfered with by the presence of I_3^- if it is present [initial portions of all traces (a–d) and the final portions of traces (b–d)]. Initial concentrations are [Tyr], 324 μ M; $[H_2O_2]$, 1.02 mM; [LPO], 1.14 μ M with varying concentration of KI: (a) $[KI]/[Tyr] = 4.5$; (b) $[KI]/[Tyr] = 5.0$; (c) $[KI]/[Tyr] = 5.5$; (d) $[KI]/[Tyr] = 6.0$.

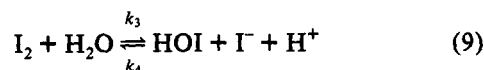
DISCUSSION

Although peroxidases are generally considered to catalyze oxidation in a similar manner and to be relatively nonspecific with regard to substrates, closer investigation shows striking differences. The present investigation shows that lactoperoxidase is more efficient than horseradish peroxidase in its ability to catalyze iodide oxidation and much more efficient in its ability to catalyze iodination of tyrosine.

HRP Mechanism. With respect to the HRP iodination system, the initial rate of I_2 formation was found to be unaffected by the presence of tyrosine (Table II). This indicates that the species resulting from iodide oxidation, in which the iodine is in a +1 oxidation state, reacts much faster with excess I^- to form the I_2 than with the tyrosine to form MIT. Molecular iodine is known to be in equilibria with other species in aqueous solution as shown in eqs 2 and 9:



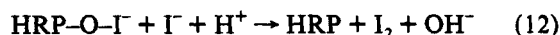
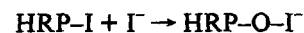
where $k_1 = (6.2 \pm 0.8) \times 10^9 \text{ M}^{-1} \text{ s}^{-1}$ and $k_2 = (8.5 \pm 1.0) \times 10^6 \text{ s}^{-1}$ (Turner et al., 1972).



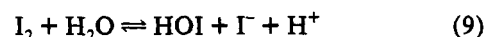
The overall rate constant for the forward reaction, k_3 , is 3.0 s^{-1} , k_4 is $4.4 \times 10^{12} \text{ M}^{-2} \text{ s}^{-1}$ for the reverse reaction (Eigen & Kustin, 1962), and the equilibrium constant K_9 is $5.4 \times 10^{-13} \text{ M}^2$ at 25.0°C (Allen & Keefer, 1955). From K_9 one can calculate the value of $[HOI][I^-]/[I_2]$ at any pH, and at pH 3.6 it is $2.2 \times 10^{-9} \text{ M}$: strong supporting evidence for our contention that I_2 is the predominant species of iodine. It is shown clearly in Figure 5b that I_3^- is not involved in the

iodination reaction at all. Thus, the depletion of I_2 , shown in Figure 6, is due to iodination of tyrosine by either I_2 or HOI , which cannot be distinguished because of the equilibrium in eq 9. Therefore, in the case of HRP, either I_2 or HOI is the iodinating reagent. The pseudocatalytic degradation of H_2O_2 by iodide and HRP was observed by detection of O_2 evolution. The following overall mechanism is proposed for the reaction of I^- , H_2O_2 , and tyrosine in oxygenated aqueous solution catalyzed by HRP.

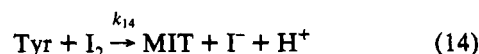
HRP reactions:



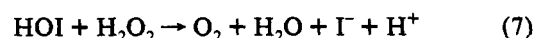
Iodine equilibria:



Nonenzymatic Iodination, one or both of the following:



Oxygen evolution:



$HRP-O-I^-$ is the enzyme-bound hypiodite which is not detected in any of our experiments and which must have a

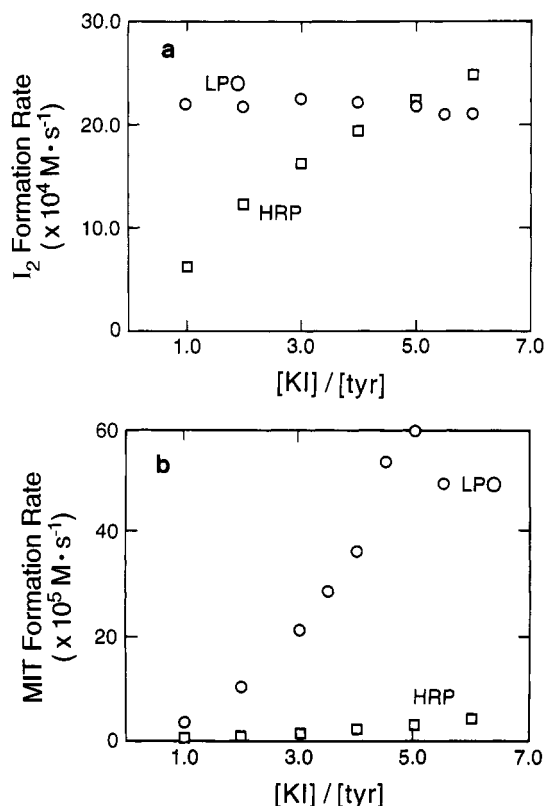


FIGURE 11: (a) Plots of initial formation rates of I₂ versus the [I⁻]/[Tyr] ratio in both the HRP and LPO iodination systems. The initial formation rates of I₂ were obtained as shown in Figure 8. One cuvette contained H₂O₂ and KI in citrate buffer of ionic strength 0.11 M, pH 3.50 (for HRP) or pH 4.97 (for LPO); the other contained HRP or LPO and tyrosine in K₂SO₄ solution of ionic strength 0.11 M. (b) Plots of monoiodotyrosine formation rates which were obtained as shown in Figure 9 versus the [KI]/[Tyr] ratio. Experimental conditions are as in panel a.

Table III: Stereoisomeric Effect of D- and L-Tyrosine on the Initial Rates of I₂ and MIT Formation for LPO^a

[I ⁻] (mM)	I ₂ formation rate (× 10 ³ M s ⁻¹)		MIT formation rate (× 10 ⁴ M s ⁻¹)	
	L-Tyr	D-Tyr	L-Tyr	D-Tyr
0.324	2.20	2.95	0.37	0.20
0.648	2.16	3.00	1.04	0.50
0.972	2.25	2.94	2.15	1.08
1.30	2.21	2.78	3.66	1.84
1.62	2.16	2.77	5.98	3.02
1.78	2.10	2.83	4.99	3.95

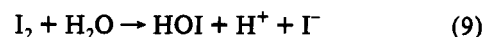
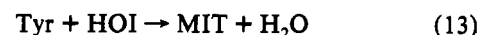
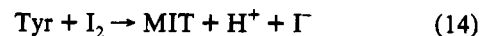
^a [LPO], 1.14 μM; [H₂O₂], 1.02 mM; [L-Tyr] or [D-Tyr] 324 μM.

very short half-life. However, it provides the only reasonable mechanism for HOI formation.

The maximum rate constants of eqs 13 and 14 can be obtained by assuming that only one of the reactions occurs for iodination. The HOI concentration at time of 1.0 s when MIT starts forming (Figure 4c) can be calculated from eq 9 by the known concentrations of I₂ and I⁻ at that time (Figure 5b). The calculated k_{13} is $9.3 \times 10^5 \text{ M}^{-1} \text{ s}^{-1}$, which is same as the result of $9 \times 10^5 \text{ M}^{-1} \text{ s}^{-1}$ obtained by Dunford and Ralston (1983), and k_{14} is $1.18 \times 10^4 \text{ M}^{-1} \text{ s}^{-1}$. There is approximately 2 orders of magnitude difference between the two rate constants. Since there is an equilibrium between I₂ and HOI (eq 9), one cannot distinguish which of the nonenzymatic species, I₂ or HOI, is responsible for tyrosine iodination when HRP is the catalyst for their formation.

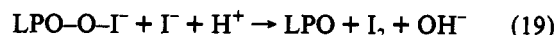
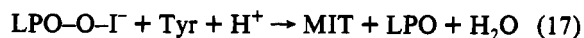
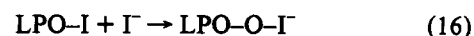
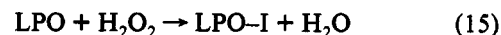
LPO Mechanism. In the case of lactoperoxidase, the experimental results clearly show that the initial rate of I₂

formation is decreased by the presence of tyrosine (Table II). Also, the initial rate of MIT formation occurs in the absence of I₃⁻ formation (Figure 10). If nonenzymatic iodination were occurring in this region, either through I₂ or HOI, then either of the following mechanisms of formation of I₃⁻ would occur:

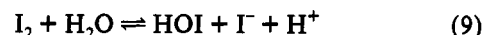


The combination of either eqs 14 and 2 or eqs 9, 13, and 2 leads to I₃⁻ formation, which is not occurring in the initial region, but only after H₂O₂ is exhausted. This indicates that the initial tyrosine iodination must take place through the LPO-bound hypoiodite complex (LPO-O-I⁻). The initial rate of MIT formation catalyzed by LPO is about 10 times faster than by the HRP system (depending somewhat on the [KI]/[Tyr] ratio) as shown in Figure 11b. This provides further evidence that the LPO-bound hypoiodite complex serves as an iodinating species which is a much more efficient iodinating reagent than either I₂ or HOI. At the same time, it was observed that the rate of I₂ formation remains significant. Therefore, nonenzymatic iodination becomes important in later stages of the reaction and is the only mechanism of iodination when H₂O₂ is exhausted. The mechanism of catalysis for LPO is summarized in the following equations:

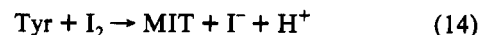
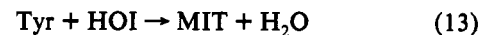
LPO reactions:



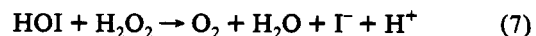
Iodide equilibria:



Nonenzymatic iodination, one or both of the following:



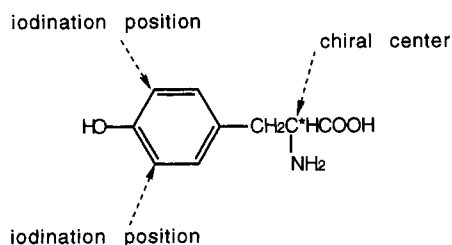
Oxygen evolution:



Over a wide range, the rate of I₂ formation is independent of the initial I⁻ concentration (Figure 11a), whereas at sufficiently low I⁻ concentrations, it is dependent (data not shown). This phenomenon can be explained by eqs 16, 18, 19, and 9. At low I⁻ concentrations, eq 16, 19, or 9 is the rate-determining step; therefore, the rate of I₂ formation is dependent on I⁻ concentration. However, when I⁻ concentration is increased, the rates of eqs 16, 19, and 9 are increased, so that eq 18 becomes the rate-determining step which is independent of the I⁻ concentration.

Our results on the iodination of D-tyrosine are in contrast to those of Morrison and Bayse (1970) who claimed that

D-tyrosine is more reactive. Our results indicate that the LPO-catalyzed tyrosine iodination reaction has some stereospecificity under our experimental conditions. Therefore, tyrosine is bound to LPO when the iodination reaction occurs. This is further evidence that the LPO-bound hypoiodite complex is responsible for the iodination of tyrosine. Nevertheless, the D-isomer still has significant reactivity which can be explained because of the large distance between the chiral carbon center and the iodination positions.



Conclusions. The data reported in the present study indicate that either I_2 or HOI is the iodinating species in the HRP iodination system. The role of HRP is to catalyze the formation of HOI, which reacts with excess I^- to form I_2 . Thus in the HRP system the actual iodination step is nonenzymatic. For the mammalian enzyme, an LPO-bound hypoiodite complex, LPO-O- I^- , is an efficient iodinating species and under physiological conditions is probably the only iodinating reagent. Under our experimental conditions, either I_2 or HOI also is important in later stages of the reaction. While it is impossible to make a choice, based exclusively on kinetic data, between HOI and I_2 as nonenzymatic iodinating reagents, there is a good physiological reason to favor HOI. Our data show that its rate constant for reaction with tyrosine is about 100 times larger than that for I_2 . Therefore, about a 200-fold lower initial concentration of iodide would lead to the same rate of formation of MIT from HOI as one would obtain from I_2 . This also fits a picture of the simplest evolutionary progression: from use of HOI free in solution to enzyme-bound hypoiodite as the iodinating reagent.

REFERENCES

- Allen, T. L., & Keefer, R. M. (1955) *J. Am. Chem. Soc.* 77, 2957-2960.
- Awtrey, A. D., & Connick, R. E. (1951) *J. Am. Chem. Soc.* 73, 1842-1843.
- Bayse, G. S., & Morrison, M. (1971) *Arch. Biochem. Biophys.* 145, 143-148.
- Cotton, M. L., & Dunford, H. B. (1973) *Can. J. Chem.* 51, 582-587.
- Davidson, B., Neary, J. T., Strout, H. V., Maloof, F., & Soodak, M. (1978) *Biochim. Biophys. Acta* 522, 318-326.
- Davies, M., & Gwynne, E. (1952) *J. Am. Chem. Soc.* 74, 2748-2752.
- Dunford, H. B., & Ralston, I. M. (1983) *Biochem. Biophys. Res. Commun.* 116, 639-643.
- Eigen, M., & Kustin, K. (1962) *J. Am. Chem. Soc.* 84, 1355-1361.
- Huber, R. E., Edwards, L. A., & Carne, T. J. (1989) *J. Biol. Chem.* 264, 1381-1386.
- Huwiler, M., & Kohler, H. (1984) *Eur. J. Biochem.* 141, 69-74.
- Huwiler, M., Bürgi, U., & Kohler, H. (1985) *Eur. J. Biochem.* 147, 469-476.
- Kohler, H., Taurog, A., & Dunford, H. B. (1988) *Arch. Biochem. Biophys.* 264, 438-449.
- Magnusson, R. P., & Taurog, A. (1983) *Biochem. Biophys. Res. Commun.* 112, 475-481.
- Magnusson, R. P., Taurog, A., & Dorris, M. L. (1984a) *J. Biol. Chem.* 259, 13783-13790.
- Magnusson, R. P., Taurog, A., & Dorris, M. L. (1984b) *J. Biol. Chem.* 259, 197-205.
- Morrison, M., & Bayse, G. S. (1970) *Biochemistry* 9, 2995-3000.
- Ohlsson, P.-I., & Paul, K.-G. (1976) *Acta Chem. Scand.* B30, 373-375.
- Paul, K.-G., & Ohlsson, P.-J. (1985) in *The Lactoperoxidase System* (Pruitt, K. M., & Tenovuo, Y. O., Eds.) Vol. 27, pp 15-30, Dekker, New York.
- Palmer, D. A., Ramette, R. W., & Mesmer, R. E. (1984) *J. Solution Chem.* 13, 673-683.
- Pommier, J., Sokoloff, L., & Nunez, J. (1973) *Eur. J. Biochem.* 38, 497-506.
- Ralston, I., & Dunford, H. B. (1978) *Can. J. Biochem.* 56, 1115-1119.
- Ramette, R. W., & Sandford, R. W., Jr. (1965) *J. Am. Chem. Soc.* 87, 5001-5005.
- Roman, R., & Dunford, H. B. (1972) *Biochemistry* 11, 2076-2082.
- Taurog, A. (1970) *Arch. Biochem. Biophys.* 139, 212-220.
- Thomas, J. A., & Hager, L. P. (1969) *Biochem. Biophys. Res. Commun.* 35, 444-450.
- Turner, D. H., Flynn, G. W., Sutin, N., & Beitz, J. V. (1972) *J. Am. Chem. Soc.* 94, 1554-1559.
- Wren, J. C., Paquette, J., Sunder, S., & Ford, B. L. (1986) *Can. J. Chem.* 64, 2284-2296.